Anal. Chem. **2010,** *82,* 136–144

Quantitative Multiplex Detection of Pathogen Biomarkers on Multichannel Waveguides

Harshini Mukundan,[†] Hongzhi Xie,[†] Dominique Price,[†] Jessica Z. Kubicek-Sutherland,[†] W. Kevin Grace,[†] Aaron S. Anderson,[†] Jennifer S. Martinez,[‡] Nile Hartman,[§] and Basil I. Swanson*[,||]

Physical Chemistry and Applied Spectroscopy, Chemistry Division, Center for Integrated Nanotechnologies, and Chemical and Laser Science Technology, Los Alamos National Laboratory, Los Alamos, New Mexico 87545, and nGimat, Atlanta, Georgia 30341

No single biomarker can accurately predict disease. An ideal biodetection technology should be capable of the quantitative, reproducible, and sensitive detection of a limited suite of such molecules. To this end, we have developed a multiplex biomarker assay for protective antigen and lethal factor of the *Bacillus anthracis* lethal toxin using semiconductor quantum dots as the fluorescence reporters on our waveguide-based biosensor platform. The platform is extendable to a wide array of biomarkers, facilitating rapid, quantitative, sensitive, and multiplex detection, better than achievable by conventional immunoassay. Our assay allows for the sensitive (limit of detection 1 pM each), specific (minimal nonspecific binding), and rapid (15 min) detection of these biomarkers in complex biological samples (e.g., serum). To address the issue of reproducibility in measurement and to increase our sample throughput, we have incorporated multichannel waveguides capable of simultaneous multiplex detection of biomarkers in three samples in quadruplicate. In this paper, we present the design, fabrication, and development of multichannel waveguides for the simultaneous detection of lethal factor and protective antigen in serum. Evaluation of the multichannel waveguide shows an excellent concordance with single-channel data and effective, simultaneous, and reproducible measurement of lethal toxins in three samples.

Biomarkers are loosely defined as biomolecules that are differentially expressed during disease. In infectious disease, these may be pathogen-associated molecules that are secreted in the host. In cancer, these are host molecules whose expression levels are changed during disease. In either case, the differential expression of biomarkers is indicative of disease. Often, the secretion or expression of these biomarkers supersedes other pathological changes in the host, potentially allowing for very early detection of the disease. Despite these advantages, biomarkers are not routinely used for disease detection for several reasons: (1) circulating concentrations of biomarkers are very low, requiring ultrasensitive detection technology, (2) most detection platforms are influenced by nonspecific interactions in complex biological samples such as serum and urine, (3) most of the available technologies are not capable of accurate quantitation of biomarker concentrations, and (4) no single biomarker can be used for accurately predicting disease in all stages of infection. These problems have limited the development of biomarker-based detection strategies. Indeed, many of the popular diagnostic assays (e.g., the EliSpot test for tuberculosis) measure the immune response of the host to secreted pathogen biomarkers because the former is easier to measure and quantitate. An ideal biomarker-based detection strategy should be capable of the simultaneous and ultrasensitive detection of a limited suite of such biomolecules in complex biological samples. The work presented in this paper addresses many of the limitations of biomarker-detection strategies.

Planar optical waveguides are comprised of a thin optically transparent film with a refractive index higher than that of the adjacent substrate and have extensively been exploited in biological and chemical sensing systems.[1] Both research and commercial technologies are known that work in conjunction with one of several different transduction schemes such as fluorescence, interferometry, and radiolabeling. Waveguide-based biological sensors and differential transduction schemes have both been extensively reviewed.[1,2] The sensor team at the Los Alamos National Laboratory has developed a waveguide-based optical biosensor platform for the sensitive and specific detection of biomarkers associated with disease. We have previously validated the application of this technology to the detection of biomarkers associated with diseases such as anthrax,[3,4] influenza,[5] breast

* To whom correspondence should be addressed. E-mail: basil@lanl.gov. Phone: (505) 667-5814.

[†] Physical Chemistry and Applied Spectroscopy, Chemistry Division, Los Alamos National Laboratory.

[‡] Center for Integrated Nanotechnologies, Los Alamos National Laboratory.

[§] nGimat.

[||] Chemical and Laser Science Technology, Los Alamos National Laboratory.

(1) Mukundan, H.; Anderson, A. S.; Grace, W. K.; Grace, K. M.; Hartman, N.; Martinez, J. S.; Swanson, B. I. *Sensors* **2009**, *9*, 5783–5809.

(2) Li, S.; Amstutz, P., II; Tang, C.; Hang, J.; Xhu, P.; Zhang, Y.; Shelton, D.; Karns, J. S. *Meth. Mol. Biol: Biosens. Biodetect.* **2008**, *503*, 389–401.

(3) Martinez, J. S.; Grace, W. K.; Grace, K. M.; Hartman, N.; Swanson, B. I. *J. Mater. Chem.* **2005**, *15*, 4639–4647.

(4) Mukundan H.; Xie H.; Anderson A. S.; Grace W. K.; Martinez J. S. Swanson B. I. *BiOS; Frontiers in Pathogen Detection: From Nanosensors to Systems*, San Jose, CA; SPIE: San Jose, CA., 2009; pp 71670A-1−71670A-10.

(5) Kale, R.; Mukundan, H.; Price, D.; Foster-Harris, J.; Lewallen, D. M.; Swanson, B. I.; Schmidt, J. G.; Iyer, S. S. *J. Am. Chem. Soc.* **2008**, *130* (26), 8169–8171.

10.1021/ac901497g
Published on Web 12/11/2009

cancer,[6,7] and tuberculosis (unpublished data). The exponential decay of the evanescent wave within 200−400 nm from the waveguide surface allows for spatial filtering, thereby minimizing autofluorescence associated with complex samples such as serum. By this mechanism, only molecules bound on the waveguide surface are excited, whereas fluorescent solution contaminants are not detected. This allows for the minimization of nonspecific interactions, especially when complex biological samples, which may be autofluorescent, are considered. Further, we have developed optimal silane-based surfaces for waveguide functionalization that minimize nonspecific binding in complex patient samples.[8] Additionally, we have successfully evaluated our technology for the detection of breast cancer biomarkers in patient serum and nipple aspirate fluid samples and obtained 100% corroboration with disease progression in a blind study.[6]

Accurate detection diagnosis requires simultaneous detection of a suite of biomarkers. Therefore, an ideal detection strategy should be capable of the sensitive detection of a limited suite of such biomolecules. We have attempted to achieve multiplex detection by using photostable and tunable quantum dots (QDs) as the fluorescence reporters in our experimental platform. QDs have been used for a variety of biological applications such as DNA sorting, measuring protein−protein interactions, enzyme assays, and *in situ* hybridization experiments.[9] Compared to organic dyes, QDs provide several advantages that make them amenable for use in an immunoassay platform. QDs have broad absorption bands with high extinction coefficients, narrow and symmetric emission bands with high quantum yields, and excellent photostability.[10] Perhaps the most significant advantages of QDs to multiplex detection platforms is their broad Stokes shift, which facilitates the simultaneous excitation of several distinct QDs at a single excitation wavelength.[10−13] The size-based optical "tunability" of QDs, when combined with their other advantages, makes them ideal candidates for use in biological applications such as ours. Indeed, it has been said that "multiplex detection platforms is where QDs will have their maximum application in the near future".[14] More recently, antibodies conjugated with dihydroxylipoic acid capped QDs have been used in plate-based immunoassays for protein toxins.[14] The investigators were able to achieve the simultaneous detection of four protein toxins with reasonable sensitivity using this approach. However, this technology suffers from the drawbacks of traditional plate-based immunoassays such as poor sensitivity, high nonspecific binding, and insufficient quantitation. Further, DHLA QDs are associated with low quantum efficiency and are unstable at neutral pH, limiting their application to bioassays in general. In this study, we have attempted to overcome these disadvantages by (1) performing the immunoassays on a functionalized waveguide, thereby allowing for excellent sensitivity, low nonspecific binding, and accurate quantitation, and (2) using polymer-coated QDs that are stable at neutral pH and hence better suited for biological applications.

To facilitate assay reproducibility and to increase the throughput of samples processed at a given time, we have developed a multichannel waveguide capable of the simultaneous detection of three different samples in quadruplicate. Herein we report, for the first time, the design, fabrication, and evaluation of a multichannel waveguide for the sensitive, quantitative, multiplex detection of *Bacillus anthracis* antigens—protective antigen (PA) and lethal factor (LF)—in serum using QDs as the fluorescence reporters. Streptavidin-coated QDs were used as an internal standard to measure inter- and intraassay variability. These biomarkers are simply a model system for the demonstration of the feasibility of this detection approach. In theory, the assay can be used for any biomarker for which two recognition ligands are available.

EXPERIMENTAL SECTION

Materials. Waveguides were fabricated at nGimat, Atlanta (see the Methods). Purified antibodies (mouse monoclonal, IgG1, human adsorbed) that bind orthogonal epitopes of the anthrax PA and LF were obtained from QED Bioscience Inc. Amino-functionalized QDs (655 nm, QD655), Qdot655 ITK carboxyl QDs, AF647-*N*-hydroxysuccinimide (NHS) ester labeling kits, streptavidin−QD conjugate (S−QD565), and 96-well plates were purchased from Invitrogen. Purified protective antigen and lethal factor were obtained from the RDI Division of Fitzgerald Industries and stored at −80 °C until use. Biotinylation, protein estimation, and electrophoresis reagents were obtained from Pierce. Gel filtration columns and spin filters were from Harvard Apparatus. Buffers and membrane spin filters were from Millipore Inc., and chemicals, immunoblot materials, and other components were purchased from Sigma-Aldrich or Fisher Scientific. Materials required for waveguide functionalization are listed in detail elsewhere.[8] Nunc Immunosorp plates for use in immunoassays were purchased from Nalgene Nunc Inc. (Milwaukee, WI). Secondary antibodies were purchased from Jackson ImmunoResearch, West Grove, PA, and Southern Biotech Ltd., Birmingham, AL. All other immunoassay and protein estimation reagents were purchased from Pierce Biologicals Ltd., Rockford, IL.

Methods. *Design, Composition, and Fabrication of Waveguides.* The fabrication and specification of single-mode planar optical waveguides used in our assay are described in detail elsewhere.[3,6,15] The specifications of the multichannel waveguide were developed at the Los Alamos National Laboratory, and the waveguides were generated at nGimat, Atlanta. The waveguide consists of a 76.2 mm diameter, 2 mm thick fused silica optically polished substrate

(6) Mukundan, H.; Kubicek, J. Z.; Holt, A.; Shively, J. E.; Martinez, J. S.; Grace, K.; Grace, W. K.; Swanson, B. I. *Sens. Actuators, B* **2009**, *138* (2), 453–460.

(7) Mukundan, H.; Xie, H.; Anderson, A. S.; Grace, W. K.; Shively, J. E.; Swanson, B. I. *Bioconjugate Chem.* **2009**, *20* (2), 222–230.

(8) Anderson, A. S.; Dattelbaum, A. M.; Montano, G. A.; Price, D.; Schmidt, J.; Martinez, J. M.; Grace, W. K.; Grace, K.; Swanson, B. I. *Langmuir* **2008**, *24* (5), 2240–2247.

(9) Jamieson, T.; Bakhshi, R.; Petrova, D.; Pocock, R.; Imani, M.; Seifalian, A. M. *Biomaterials* **2007**, *28* (31), 4717–4732.

(10) Michalet, X.; Pinaud, F. F.; Bentolila, L. A.; Tsay, J. M.; Doose, S.; Li, J. J.; Sundaresan, G.; Wu, A. M.; Gambhir, S. S.; Weiss, S. *Science* **2005**, *307* (5709), 538–544.

(11) Winter, P. M.; Caruthers, S. D.; Kassner, A.; Harris, T. D.; Chinen, L. K.; Allen, J. S.; Lacy, E. K.; Zhang, H.; Robertson, J. D.; Wickline, S. A.; Lanza, G. M. *Cancer Res.* **2003**, *63*, 5838–5843.

(12) Medintz, I. L.; Uyeda, H. T.; Goldman, E. R.; Matoussi, H. *Nat. Mater.* **2005**, *4* (6), 435–446.

(13) Jaiswal, J. K.; Mattoussi, H.; Mauro, J. M.; Simon, S. M. *Nat. Biotechnol.* **2003**, *21* (1), 47–51.

(14) Goldman, E. R.; Clapp, A. R.; Anderson, G. P.; Uyeda, H. T.; Mauro, J. M.; Medintz, I. L.; Mattoussi, H. *Anal. Chem.* **2004**, *76* (3), 684–688.

(15) Grace, K. M.; Goeller, R. M.; Grace, W. K.; Kolar, J. D.; Morrison, L. J.; Sweet, M. R.; Wiig, L. G.; Reed, S. M.; Lauer, S. A.; Little, K. M.; Bustos, G. L.; Anderson, A. S.; Swanson, B. I. *Proc. SPIE—Int. Soc. Opt. Eng.* **2004**, 55–64.

(low refractive index, μ =1.46) and a Si_3N_4 high-index film (μ = 1.81), 110 nm ± 5 nm thick. The very thin film requires the use of refractive grating elements for coupling light into the waveguide. The grating coupler elements are fabricated using a holographic interference technique to generate the periodic pattern prior to the deposition of the waveguide film. For a wavelength of 532 nm and a +10° coupling angle the period is 420 nm. That pattern is etched into the substrate surface by a reactive ion etching process and subsequently overcoated with the Si_3N_4. To ensure the gratings are not affected by ambient refractive index changes, the grating coupler region must also be overcoated with a layer of dense SiO_2 (1100 nm or thicker), thus isolating the evanescent field from the surrounding media. The actual sensing area is a thin (10 nm) SiO_2 film that is deposited on the Si_3N_4 film on the waveguide surface sensing area, which provides the functional surface required for the attachment of self-assembled monolayer or lipid bilayer sensing films.

The multichannel waveguide consists of three channels with four sensing elements per channel (Figure 1). Each sensing element is 10 mm long and 1.5 mm wide and has a 1.5 mm × 1.5 mm detractive grating element, which enables independent excitation of each sensing element. The channels and sensing elements also have a chrome absorbing material surrounding them, which removes the possibility of cross-talk or inadvertent coupling between the sensing elements. After the waveguide coatings have been deposited onto the substrate, the substrate is cut to its final dimensions (76.2 mm × 25.4 mm). Cutting the substrate to these dimensions permits it to be incorporated into a flow cell (specifically designed for these waveguides) and mounted into a holder for use on our waveguide-based optical biosensor (Figure 1). The design and fabrication of the multichannel waveguide allows for accurate detection in all 12 sensing elements without any fluorescence bleed-through. The injection time is very short (a few seconds) with respect to the diffusion time for antigens and reporter antibodies in the injected sample. As a result, each element "sees" the same concentration of target antigens and reporter antibodies. For experiments using a single exposure of sample to the sensing chip, as described below, the total analyte contained within the sample is $\sim 1 \times 10^{-17}$ mol for the limit of detection (LoD = 1 pM) noted below for PA and LF.

Waveguide Functionalization and Flow Cell Assembly. The waveguide surface is functionalized using self-assembled monolayers (SAMs) as is described in detail elsewhere.[8] Briefly, silica surfaces were functionalized by self-assembly of an amine-terminated silane film using vapor-phase deposition of (3-aminopropyl)methyldiethoxysilane. The quality of the monolayer films and uniform surface coverage was determined by ellipsometry and contact angle measurements. The amine-terminated films were chemically modified with a mixture of carboxylic acid-terminated poly(ethylene glycol) (PEG) chains of varying functionality. A fraction of the PEG chains (0.1−10 mol %) were terminated in biotin, which produced a surface with an affinity toward streptavidin. The surface is biotinylated (0.1%) to facilitate the immobilization of a biotinylated capture antibody by biotin−avidin chemistry and allows for the use of a QD-labeled streptavidin, with an emission at 565 nm (S−QD565), as the internal standard.

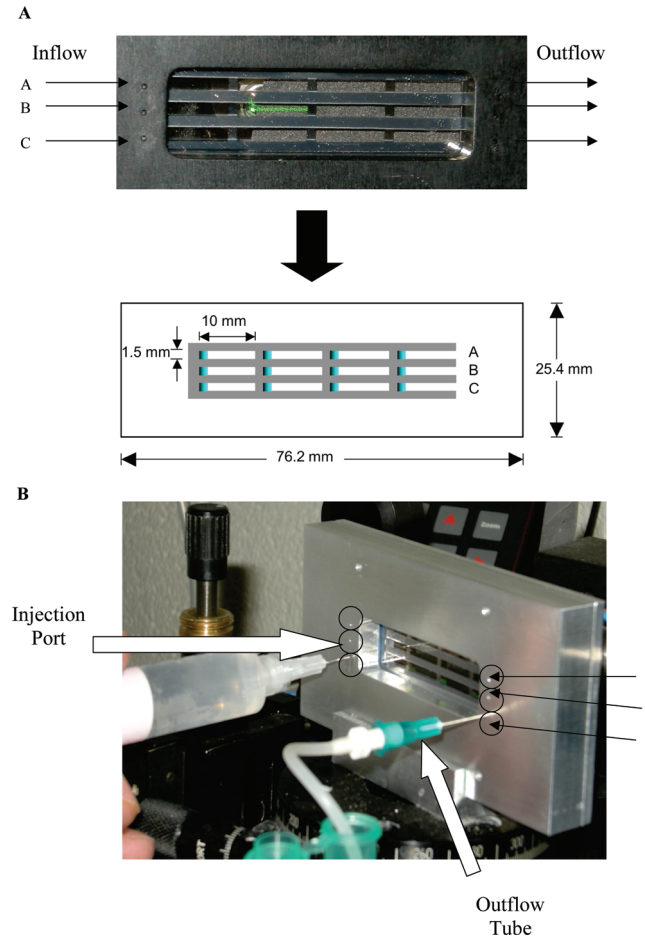

Figure 1. (A) (Top) Photograph of the multichannel waveguide assembled in a flow cell. Laser light (532 nm excitation) is coupled into grating B2. The bright spot is the incident laser beam being coupled into the waveguide via the refractive holographic grating coupling element, and the streak to the right is the propagation of the in-coupled light by total internal reflection. (Bottom) Schematic representation of the multichannel waveguide (not to scale). Dimensions of the individual sensing elements are indicated. The colored squares represent the refractive holographic grating couplers etched into each sensing element. The channels and sensing elements have a chrome absorbing material surrounding them, permitting each sensing element to be excited independently without cross-talk or inadvertent coupling between the sensing elements. The chrome absorbing material is represented by the gray mask surrounding each element. (B) Multichannel waveguide assembled in a specially designed flow cell, which allows the waveguide to be mounted to the instrument and the ability to inject samples into each channel independently. Flow channels A, B, and C are indicated by the black circles. The injection port and outflow tube are shown. In this case, the outflow is out of channel C.

The functionalized single-channel waveguides are assembled into a flow cell.[5] The functionalized multichannel waveguides require different materials. The flow cell consists of a three-channel (0.5 mm thick) silicone rubber gasket and a glass cover (76.2 mm × 25.4 mm × 1 mm) with six holes precisely bored to align individual channels (Figure 1). In either single-channel or multichannel arrangements, the flow cell is mounted onto a holder with septum material over the holes. The septa form a seal with the glass cover and allow the addition of reagents via a syringe. This configuration minimizes reagent volumes (100 μL/channel), is self-sealing, and allows the addition of multiple reagents.

Fluorescence-Based Sandwich Immunoassay on the Waveguide Surface. Preparation of Antibodies. Antibodies that bind orthogonal epitopes of PA and LF were identified from either previous work in our laboratory[3] or the literature.[16] The detailed protocols for the biotinylation of the capture antibody[7] have been described elsewhere. Briefly, the capture antibodies were modified by biotinylation using sulfo-NHS−biotin (20 molar excess) to allow their immobilization on the waveguide surface. The antibody, in PBS, was mixed with the EZ-Link sulfo-NHS−biotin and incubated at room temperature for 50 min. Free biotin and reagents were removed by size-exclusion chromatography on a Sephadex G25 column. The biotinylated antibodies (biotin−anti-PA or biotin−anti-LF) were characterized by HABA analysis for the degree of labeling and by immunoblot for functionality as previously described.[7]

For labeling of the reporter antibodies with photostable QDs, antibodies were buffer-exchanged from PBS to borate buffer (10 mM, pH 7.3) by using 10 000 molecular weight cutoff (MWCO) spin filters. Carboxyl QD605 or QD655 stock (70 μL, 8 μM in borate buffer at pH 9.0) was diluted with 500 μL of borate buffer (10 mM, pH 7.3) and mixed with 200 μg of anti-PA or anti-LF antibody, respectively. *N*-Ethyl-*N*′-[(dimethylamino)propyl]carbodiimide (EDC) in aqueous solution (8.4 μL, 100 mM) was added, and the reaction mixture was stirred gently at room temperature for 1.5 h. The reaction was quenched by addition of borate buffer (500 μL, 50 mM, pH 9.0), incubated at 4 °C overnight, and then washed at least five times with 1 mL of borate buffer (25 mM, pH 7.5) using a 100 000 MWCO membrane spin filter. The reaction mixture was then passed through a second 1 000 000 MWCO spin filter to remove large aggregates, and the filtrate was concentrated using a 10 000 MWCO spin filter, with a final solution buffer exchange to pH 7.5. The concentration of QDs was measured on the basis of the absorbance of QD605 at 532 nm with ε_{532} = 810 000 M^{-1} cm^{-1} and QD655 with ε_{532} = 2 100 000 M^{-1} cm^{-1}. The concentration of QD-conjugated antibodies was measured using bovine serum albumin as the standard and BCA as the working reagent. Antibody−QD conjugates were characterized by SDS−polyacrylamide gel electrophoresis (12.5%) and agarose gel electrophoresis (1%) and visualized by fluorescence imaging. The molar ratio of antibody to QD in the conjugate was measured and is approximately 3:1. Purified QD-labeled antibodies (anti-PA−QD605 and anti-LF−QD655) were used as fluorescence reporters in the assay.

Evaluation of Antibody Functionality by Plate-Based Immunoassay. Both indirect and sandwich immunoassays were performed to assess antibody function and sensitivity. For enzyme-linked indirect immunoassay, 96-well Immunosorp plates were coated with PA or LF at a concentration of 2 μg/mL, and subsequently incubated with anti-PA−QD605 and anti-LF−QD655 (100 nM) in PBS−Tween 20 (0.1%) containing 4.5% fish gelatin. Following washing to remove any unbound reagents, antimouse HRP-conjugated species-specific secondary antibody was added (1:2000). We then added tetramethylbenzidine substrate and measured the absorbance at 405 nm with a plate reader. No antigen, no primary antibody, no secondary antibody, and serum controls were also performed. These preliminary experiments confirmed the bioactivity of the QD-labeled antibodies (Figure 2a,b).

For fluorescence-based sandwich immunoassays, 96-well plates were coated with the appropriate capture antibodies (see above, 100 nM) in PBS for 2 h at 37 °C. The plates were blocked with 4.5% fish gelatin in PBS−Tween 20 (0.1%) for 1 h at room temperature. The antigen (PA or LF) was then added at a concentration of 2.5 μg/mL. Following an overnight incubation at 4 °C, the reporter antibodies (anti-PA−QD606 or anti-LF−QD655) were added at a concentration of 100 nM in PBS and incubated for 2 h. QD-associated fluorescence was measured post wash using a Molecular Devices Gemini fluorescence plate reader. These experiments measured the efficacy of the QD-labeled antibodies to detect PA and LF in a plate-based format using the fluorescence readout. The LoD was determined to be ~ 0.1 nM for both antigens (Figure 2c,d).

Multiplex Detection of PA and LF on Single-Channel Waveguides and Measurement of QD Photostability. Sandwich assays for PA and LF were individually optimized on the waveguide platform before transitioning to the multiplex assay. A schematic representation of the multiplex assay is shown in Figure 3a. Application of the assays to a multiplex format required optimization of QD−antibody pairs. Several factors such as the antigen−antibody binding efficiency, quantum efficiency of the QD being used, QD size, number of antibodies conjugated on the QD surface, antibody conformation, stability of the conjugate, and assay sensitivity all affect the assay performance. Our preliminary experiments determined that conjugation of the anti-LF antibody with QD605 and the anti-PA antibody with QD655 provided a relatively lower sensitivity in a multiplex format (data not shown). We optimized the multiplex assay format using anti-PA−QD605 and anti-LF−QD655 conjugates as reporters, and a typical measurement spectrum is shown in Figure 3b. Kinetic measurements of antigen−antibody binding were also measured as a function of the antigen concentration. On the basis of these studies (data not shown), 10 min was determined as the optimal time for antigen−antibody incubation in our assay.

All experiments used a continuous-wave 532 nm diode-pumped solid-state (5 mW, power coupled into the waveguide 440 μW) frequency-doubled Nd:YAG laser for excitation. The flow cell was assembled as described before. No blocking or stabilization was required with the use of SAMs as the functional surface. All injections were 200 μL in volume and were incubated for 10 min, followed by a wash with PBS containing 0.5% BSA. In both single-channel and multichannel experiments, waveguide metrics were measured before actual sample addition. These included the waveguide background (a measure of intrinsic fluorescence associated with the impurities in the waveguide itself), power coupled upon excitation (incident power is maintained at 440 μW), and fluorescence signal associated with binding of the internal standard to the biotinylated SAM (S−QD565, 10 pM). Once these measurements were made, the biotinylated capture antibody was added (b-anti-PA or b-anti-LF or both, 100 nM each). Subsequently, nonspecific binding of the control serum and the fluorescence reporter to the functional surface was measured (anti-PA−QD605 and/or anti-LF−QD655). In multiplex experiments, the two fluorescent reporters were added sequentially (10 min incubation each) instead of together to overcome differences in measurement

(16) Geddie, M.L. O']?>; Loughlin, T. L.; Woods, K. K.; Matsumura, I. *J. Biol. Chem.* **2005**, *280*, 35641–35646.

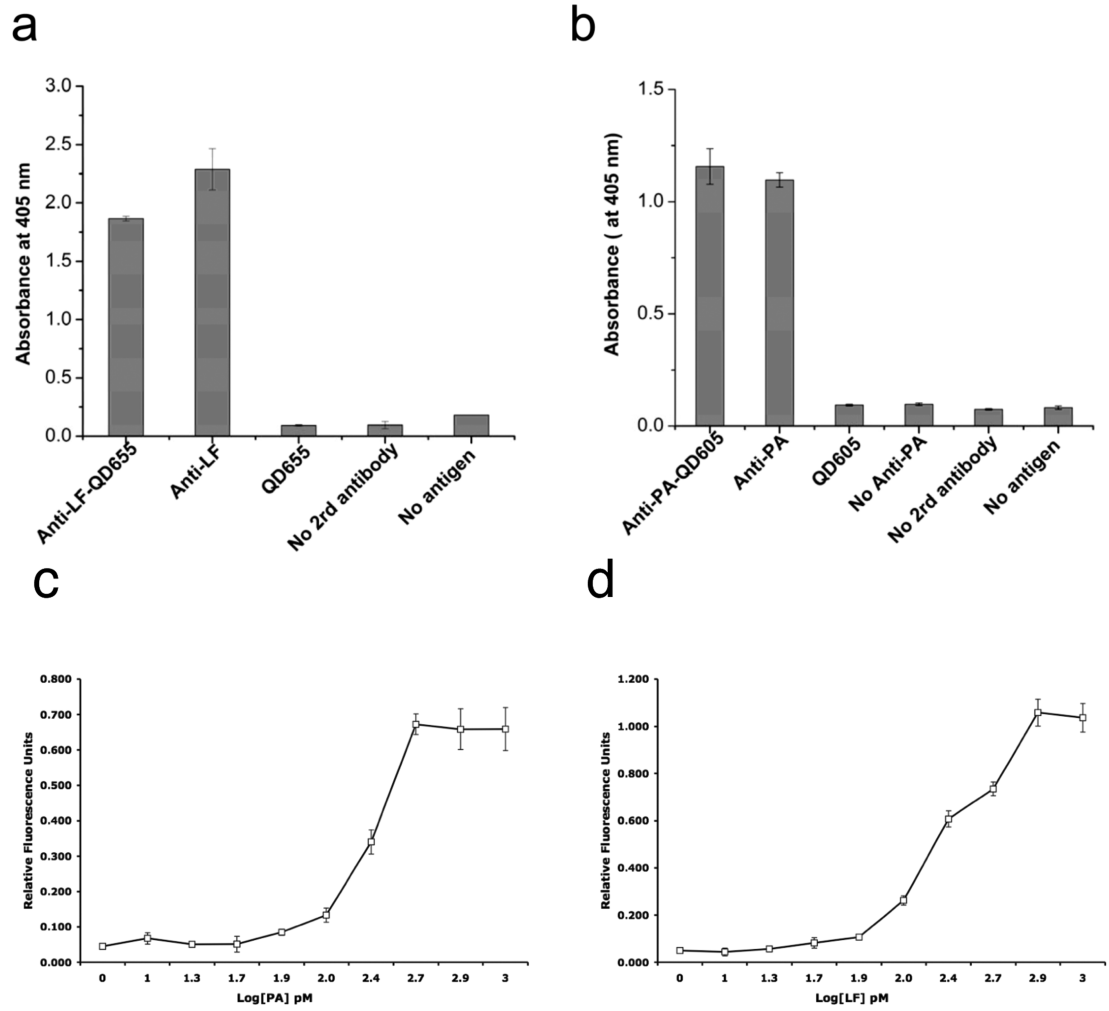

Figure 2. Activity assays for QD-labeled antibodies measured by traditional plate-based assays. Confirmation of the activity of the QD-labeled antibody conjugates for LF (left) and PA (right) by enzyme-linked immunosorbent assays is shown in (a) and (b). In each case, nonspecific binding associated with the QD alone, in the absence of the reporter (anti-HRP) antibody and the antigen, was measured as the control. Binding of the antibodies to their respective antigens validates the bioactivity of the labeled conjugate. (c) and (d) demonstrate plate-based fluorescence sandwich immunoassays for PA and LF using the labeled conjugates as reporters, plotted in a semilogarithmic plot. The LoD (see the text for details) in each case, in serum, was found to be 100 pM, higher than that achieved by the waveguide-based platform (Figure 3). All data are plotted as the mean ± standard deviation of three independent measurements.

associated with variable diffusion of the two antibodies. The tunability of the QDs to emit at different wavelengths is a function of their size. Hence, QD605 is smaller than QD655. To avoid any effect of this on the observed signal, the antibodies were added in sequence. A separate set of experiments were performed (data not shown) to show that repeat addition of the fluorescence reporter (5×) does not result in a further increase in nonspecific binding. Measurement of nonspecific binding was followed by the addition of the antigen (PA or LF or both, depending on the experiment) at variable concentrations determined by the experiment (1 pM to 1 nM). Following a 10 min incubation, the reporter antibody was added again and the fluorescence signal associated with specific binding of the antigen to the antibody was measured using the spectrometer interface. Data were reported as relative fluorescence units. For comparison of data between waveguides, S−QD565 was used as an internal standard for normalization. QDs are inherently more photostable than organic dyes and resist photobleaching, especially under low-power excitation, as was used in our experiments. The internal standard signal is evaluated during every measurement of the experiment. We have determined that 1 pM streptavidin−QD565 does not show significant photobleaching (Student's t test) following 20 measurements at 3 s integration, where the incident power is 440 μW (data not shown).

Standard curves for PA and LF were generated on different waveguides to overcome any effect of differential diffusion of the QD-labeled antibodies and a linear binding on an already modified functional surface (Figure 3c). S−QD565 internal standard was used for normalization and data comparison between different waveguides. The LoD for each antigen was found to be 1 pM in serum (Figure 3c).

Measuring S−QD565 (Internal Standard) on Multichannel Waveguides. Initial experiments to evaluate the performance of these waveguides involved the measurement of streptavidin−biotin binding. After assessment of the system metrics, S−QD565 (10−100 pM, depending on the experiment) was injected into all three flow channels and the specific signal was measured (data not shown). These measurements were repeated with streptavidin labeled with QDs of varying emission (and hence size). Preliminary measurements were made to ensure that there was no effect

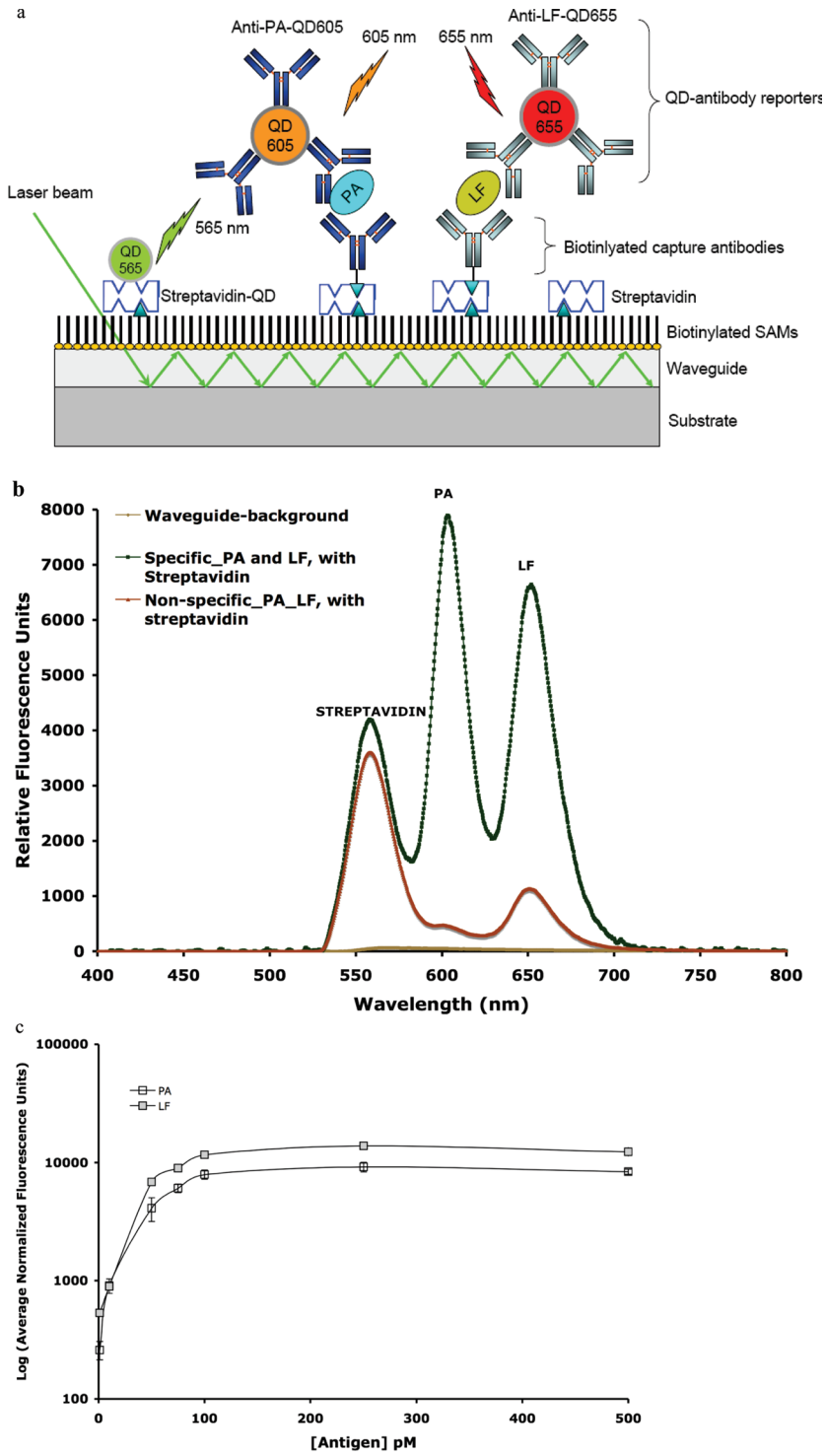

Figure 3. (a) Schematic representation of the multiplex assay on a functionalized single-channel waveguide surface. The surface is functionalized with SAMs and biotinylated anti-PA and anti-LF capture antibodies, entrapped by biotin−avidin chemistry. Some of the streptavidin (10 pM) is labeled with QD565, for use as an internal standard. Subsequent addition of the sample results in antigen (PA and LF) binding. Finally, the QD-labeled fluorescence reporters (anti-PA−QD605 and anti-LF−QD655) are added. Excitation at 535 nm results in differential emission of QDs, measured using the spectrometer interface. The multiplex spectrum obtained in a single sensing element upon detection of S−QD565, anti-PA−QD605, and anti-LF−QD655 is shown in (b). The brown line represents the waveguide background at that sensing element, which is a measure of intrinsic impurities associated with the waveguide itself and the associated scatter. This value is typically between 50 and 150 RFU for the type of waveguides used in this study. The red line indicates nonspecific binding of control serum and the fluorescently labeled reporter antibody to the functionalized waveguide surface in the absence of the antigen. The green line indicates the specific signal associated with antigen (1 pM each)−reporter binding. In both the nonspecific (red) and the specific (green) measurements, the signal associated with the internal standard (streptavidn−QD565) is also measured. A signal/noise ratio of 3.9 for LF and 1.8 for PA is observed under these conditions. Standard curves for PA and LF on the waveguide-based sensor platform as a function of the antigen concentration, plotted on a semilogarithmic scale, are shown in (c). Clear saturation at concentrations >100 pM is indicated. An LoD of 1 pM is achieved in serum, much better than the 100 pM reported with plate-based assays using the same materials (Figure 2).

on diffusion of the sample across the flow cell (data not shown). For instance, the streptavidin signals associated with channel A1 were not significantly different from those observed in channel A4. Also, reversing the flow cell orientation by changing the injection port did not affect the results (data not shown). In all experiments presented in this paper, the samples were injected in the orientation shown in Figure 1.

Multiplex Detection of PA and LF on the Multichannel Waveguide. The assay design and concentrations of reagents used for the multichannel experiments are the same as those outlined for a single channel earlier. The following experimental matrix was used: Sandwich immunoassays for PA alone were performed in flow channel B with the S−QD565 internal standard, whereas those for LF alone were performed in flow channel C. In the either case, 200 μL of serum was added to channels B and C to function as 0 pM controls. Flow channel A alone was used for multiplex detection of both antigens in the presence of the standard.

RESULTS

Evaluation of Antibody Functionality by Plate-Based Immunoassay. The detection of PA and LF by plate-based indirect and sandwich immunoassay is shown in Figure 2a,b. The indirect immunoassay used a colorimetric detection approach for measurement of PA and LF and simply allowed for the conformation of the bioactivity of the QD-labeled antibody. Parts c and d of Figure 2 demonstrate detection of PA and LF, respectively, at various concentrations between 0 and 1000 pM, plotted on a semilogarithmic scale. Assay saturation is clearly evidenced at a >250 pM concentration of either antigen. The LoD was defined as the mean of the blank + 3(standard deviation) at a confidence level of 0.95, as per the IUPAC standard definition. Using this metric, the LoD was determined to be 100 pM for each antigen.

Optimization of the Assay and Generation of Standard Curves. The multiplex assay was optimized for speed, sensitivity, quantum efficiency of the QDs, and other parameters. For example, initial iterations of the assay used an anti-LF antibody conjugated to QD605. However, the diminished quantum efficiency of QD605 and the poor binding affinity of the antibody resulted in a poor signal/background ratio (data not shown). The anti-PA reporter antibody has an inherently better binding affinity to the antigen, as was determined by plate-based assays. Therefore, combining the antibody with the better binding affinity with the QD with poorer efficiency may still result in a significant signal resolution in the assay. Following this reasoning, in subsequent experiments, the anti-LF antibody was conjugated to QD655, greatly improving the signal/background ratio. Also, the assay conditions (buffers, incubation times, order of injection) were altered to enhance the performance of the LF assay. The optimized assay, using anti-LF−QD655 and anti-PA−QD605, is indicated in Figure 3b. This assay format was used in all subsequent experiments.

The AlexaFluor-647-labeled counterpart is completely photobleached under these conditions (data not shown). This photostability is essential for quantitative multiplex assays using our approach as multiple excitations must be used to measure laser light in-coupling via the internal streptavidin standard (below).

Figure 3b demonstrates the raw spectra observed for the simultaneous detection of 1 pM PA and LF with the S−QD565 control (10 pM) in a single element of the multichannel waveguide. The waveguide-associated background is minimal (~100 RFU). The nonspecific background associated with the LF antibody (2691 RFU) is much higher than that observed with PA (405 RFU), yet the specific signal observed with antigen binding is higher (10619 RFU for LF and 703.2 RFU for PA) at a 1 pM concentration of each antigen. A signal/nonspecific binding ratio of 3.9 for LF and 1.75 for PA is observed. Concentration-dependent responses for PA and LF were then determined on individual waveguides (Figure 3c). Because of the inherent differences in the waveguides and functional surfaces, 100% linearity in response is not expected. The LoD for PA and LF was calculated using the metrics outlined in the Experimental Section. Using this method, an LoD of 1 pM was obtained for both PA and LF using the QD-labeled antibodies on the waveguide-based platform. This is much lower than the 100 pM obtained with the same antibodies but using a plate-based approach (Experimental Section, Figure 2c,d). Sandwich immunoassays for the efficient detection of anthrax lethal toxins such as PA, LF, and edema factor are available but have a lower sensitivity than our assay.[17] In addition, these assays were not performed in complex samples such as serum, which can result in higher nonspecific binding and a compromised signal/noise ratio in plate-based assays.

Detection of Streptavidin−QDs on the Multichannel Waveguide. A schematic representation of the design of the multichannel waveguide and a photograph of the same are shown in Figure 1. Preliminary measurements of waveguide function were performed by injecting streptavidin−QD655 at 100 pM concentrations in buffer along the three flow channels. The system metrics (in-coupled power, waveguide-grating-associated background, and streptavidin signal) were measured in each of the 12 channels. A prototype data set in Table 1 shows consistency in measurement across the channels. The coefficient of variation (CV) of data within channels and between channels was calculated using the formula (standard deviation/average) × 100 and is given in Table 1. The variability in the data is directly related to different waveguide backgrounds and coupling efficiencies in the different gratings. The measurements were repeated with the injection channel reversed and using multiple QD-labeled streptavidin (data not shown), and a consistent data set was obtained. The multichannel waveguide was then used for the sandwich measurement of PA and LF.

Multiplex Quantitative Detection of PA and LF in Serum using Multichannel Waveguides. Multiplex immunoassays were performed on the multichannel waveguide for the simultaneous detection of PA and LF in serum as outlined earlier. The signals measured for the detection of 100 pM PA/LF in each of the sensing elements of the multichannel waveguide, without normalization for interassay variability, are shown in Figure 4a. This assessment was performed because waveguides are intrinsically different from each other with respect to their fabrication, ability to couple light, and refractive index. Also, the functional properties of the waveguide vary slightly with the SAM coating in the individual gratings. Hence, the observed RFU values are expected to be very different between waveguides and within the different sensing elements of the same waveguide. The signal intensity of S−QD565 also varies depending on the power coupled into the

(17) Mourez, M.; Kane, R. S.; Mogridge, J.; Metallo, S.; Deschatelets, P.; Sellman, B. R.; Whitesides, G. M.; Collier, R. J. *Nat. Biotechnol.* **2001**, *19* (10), 958–961.

Table 1. Summary Measurement of the Waveguide-Associated Background, Coupling Efficiency (Uncoupled Power 440 μW in All Channels), and the Signal Observed with 10 pM S−565QD (Internal Standard) for One Multichannel Waveguide[a]

channel	background	coupling efficiency (%)	S565QD-10 pM	av	std dev	CV (%)
A1	125	41	3750	3612.5	978.6	27.1
A2	225	32	5000			
A3	175	25	3200			
A4	190	44	2500			
B5	180	27	3250	3025	798.7	26.4
B6	210	35	3500			
B7	250	35	3600			
B8	150	48	1750			
C9	190	30	2500	3112.5	855.5	27.5
C10	200	28	4000			
C11	300	40	3800			
C12	240	48	2150			
av	203	36	3250			
std dev	46	8	882			
CV (%)	23	22	27			

[a] Average measurements for all 12 channels, for channels A, B and C, with standard deviation are shown. The CV (%) is calculated for each of these measurement groups as well.

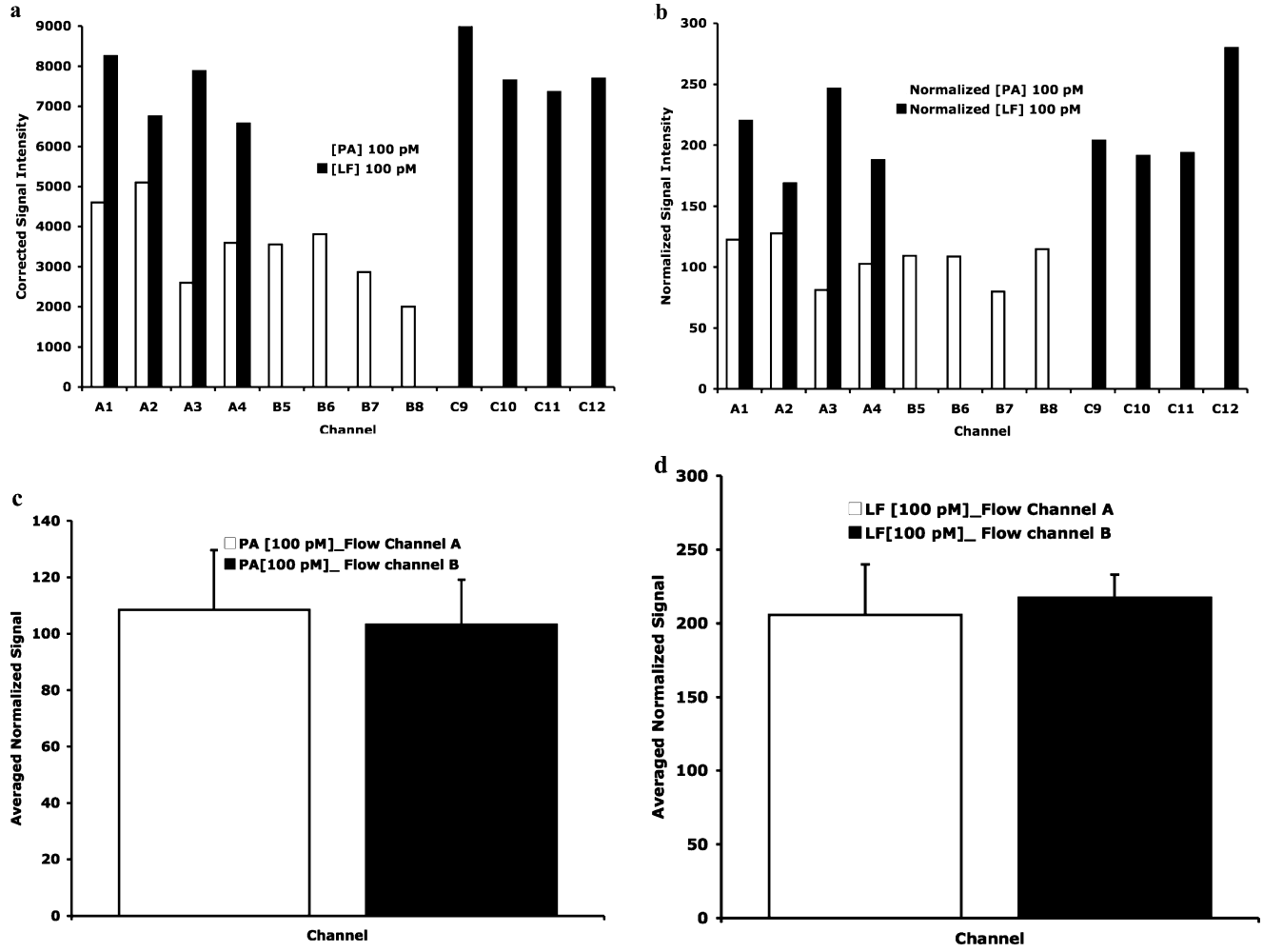

Figure 4. (a) Maximum signal intensity observed at 676 nm in all 12 grating elements with the specific detection of 100 pM PA/LF (or both) without normalization to the streptavidin standard. The data are corrected for nonspecific binding associated with the fluorescent reporter antibody and control serum. Both PA and LF were measured in channel A. Only PA was measured in channel B, and only LF was measured in channel C. Although a positive detection is achieved at this concentration in all 12 sensing elements, there is a significant variation in the signal observed. This variation is significantly reduced by normalization to the S−QD565 internal standard (b) (for statistical measurements of the CV (%), see Table 1). The average signal intensity from each channel is plotted for PA (c) and LF (d). There is no significant difference in the observed data (ANOVA with a Student−Newman−Keuls posthoc test, ($n = 4$).

Table 2. Specific Measurements for 100 pM PA and LF in the Different Channels of the Multichannel Waveguide, In a Single Experiment, before (PA and LF) and after (normalized PA and normalized LF) Normalization to the Internal Streptavidin Standard[a]

channel	PA	LF	normalized PA	normalized LF
A1	4600	8250	122.7	220.0
A2	5100	4750	127.5	168.8
A3	2597	10882	81.2	246.3
A4	3592	6570	102.6	187.7
B5	3556	0	109.4	0.0
B6	3806	0	108.7	0.0
B7	2866	0	79.6	0.0
B8	2009	0	114.8	0.0
C9	0	9180	0.0	204.0
C10	0	7650	0.0	191.3
C11	0	10360	0.0	193.7
C12	0	6690	0.0	279.6
av	3515.8	8041.5	105.8	211.4
std dev	1022.2	2062.0	17.6	36.1
CV (%)	29.1	25.6	16.6	17.1

[a] Average measurements in the eight channels for each antigen and standard deviation are calculated. The CV (%) decreases significantly with normalization to streptavidin internal standard, indicating the value of this approach.

particular sensing element and the efficiency of the SAM coating and hence can be used for normalization of the inter- and intraassay variability. As indicated in Figure 4b, much of the variability is lost when the measured signal intensities are normalized to the S−QD565 signal within that element. This observation is further supported by data in Table 2. The coefficient of variation for PA and LF measurements in the different channels is calculated before and after normalization to the internal standard. As shown in Table 2, the coefficient of variation decreases from 29.09% to 16.6% for PA with streptavidin normalization and from 27.9% to 17.05% for LF, clearly demonstrating the usefulness of the internal standard. As indicated in Figure 4c,d, the average measurements of PA and LF in serum across the different sensing elements are not significantly different from each other, as determined by a Student−Newman−Keuls posthoc ANOVA, validating the applicability of this approach for reproducible measurement of multiple samples.

These results are but the first step toward the application of multichannel waveguides to multiplex biodetection of real-world samples. Currently, SAM deposition, gasket preparation, and flow cell assembly are done manually, which requires precision and skill. We anticipate automating these processes in the future to facilitate the easy adaptation of this technology to medical diagnostics.

CONCLUSIONS

Quantitative, sensitive, specific, and rapid detection of pathogen biomarkers in complex patient samples will facilitate early detection of disease and will allow medical professionals to track the course of the disease. In this paper, we have described a step in this direction by developing multiplex detection assays on multichannel waveguides for a limited suite of disease biomarkers in complex samples. Specifically, we have shown (a) methods for the conjugation of antibodies to polymer-coated QDs with excellent control of the antibody/QD ratio and stability of these conjugates at neutral pH for bioapplications, (b) a multiplex assay for *B. anthracis* PA and LF in serum using QDs as the fluorescence reporter, with a superior LoD than is achievable with traditional plate-based assays (Figures 2 and 3), (c) design, fabrication, and development of multichannel waveguides for the detection of a limited suite of biomarkers in multiple samples (Figure 1), (d) successful evaluation of the multichannel waveguide for the simultaneous detection of PA and LF in serum, with no compromise in sensitivity by using a complex biological matrix, and (e) use of S−QD565 as an internal standard for optimization of inter- and intraassay variability. Our approach can be used for a wide variety of pathogen biomarkers, secreted in the host, as well as for malignant disease markers. The waveguide design, fabrication, and use can be modified to facilitate a higher throughout of samples with relative ease. We are currently optimizing the gasket design and flow cell construction to facilitate the application of the multichannel waveguide to evaluation of disease biomarkers in infected samples from actual patients.

ACKNOWLEDGMENT

We thank Dr. Jurgen Schmidt for many useful suggestions and helpful discussions. This work was supported by a LDRD Directed Research Award to B.I.S. and Bette Korber. This work was performed, in part, at the Center for Integrated Nanotechnologies, a U.S. Department of Energy, Office of Basic Energy Sciences, user facility at the Los Alamos National Laboratory (Contract DE-AC52-06NA25396).

Received for review July 6, 2009. Accepted November 24, 2009.

AC901497G